A New Load Torque Identification Sliding Mode Observer for Permanent Magnet Synchronous Machine Drive System

Lu, Wenqi; Zhang, Zhenyi; Wang, Dong; Lu, Kaiyuan; Wu, Di; Ji, Kehui; Guo, Liang

Published in:
IEEE Transactions on Power Electronics

DOI (link to publication from Publisher):
10.1109/TPEL.2018.2881217

Publication date:
2019

Document Version
Accepted author manuscript, peer reviewed version

This article has been accepted for publication in a future issue of this journal, but has not been fully edited. Content may change prior to final publication. Citation information: DOI 10.1109/TPEL.2018.2881217, IEEE Transactions on Power Electronics

A New Load Torque Identification Sliding Mode Observer for Permanent Magnet Synchronous Machine Drive System

Wenqi Lu, Zhenyi Zhang, Dong Wang, *member, IEEE* , Kaiyuan Lu, *member*, *IEEE*, Di Wu, Kehui Ji, and Liang Guo

***Abstract*—Effective identification of the load torque is one of the key aspects in improving the performance of servo drive systems against load disturbances. Sliding mode variable structure control has become a popular method in the development of a load torque identification (LTID) algorithm due to its parameter insensitivity and easy realization features. However, existing LTID sliding mode observers with conventional structure have the disadvantages of high frequency chattering and poor estimation accuracy, which limit its application in high performance servo systems. In this paper, the mathematical model of the conventional LTID sliding mode observer is deduced and analyzed. A new LTID sliding mode observer is proposed by replacing the sign function with a saturation function and an additional feedback loop in the load torque observer. The effectiveness of the proposed observer is verified by various experiments. The results show that compared to conventional load torque observer, the proposed observer can identify the load torque with higher accuracy and faster response in different operation conditions.**

***Index Terms*—Sliding mode variable structure control, Load torque identification, Sliding mode observer, Chattering, Robustness.**

I. INTRODUCTION

PERMANENT magnet synchronous machine (PMSM) has been widely used in various industrial, civil and military fields due to its advantages of high power factor, high efficiency, fast dynamic response, high reliability, etc. In recent years, it has gradually replaced the traditional high power asynchronous machines or hydraulic systems used in some large and high-end equipment, such as servo broaching machine [1-2], all-electric injection molding machine [3-4], crank servo press [5-6], etc. However, when the PMSM drive is used in the above-mentioned large high-end equipment, special efforts are required to suppress the speed fluctuation under operating conditions with large load and inertia variations. To achieve this, on-line load torque identification is required.

A back-stepping technique based angular position tracking controller is proposed in [7], where the load torque disturbances, frictional force and unknown dynamics are estimated by means of a reduced order observer. An adaptive speed controller is designed in [8] based on the model reference adaptive control (MRAC) method, where the observation of the load torque disturbance is achieved by carrying out the feedforward compensation. However, these methods depend on the system mathematical model and are not robust to the variation of the system parameters. Disturbance observer based control (DOBC) and related methods have been studied and applied in various industrial sectors in the last four decades [9-10]. Although the DOBC methods in [9] and [10] are able to estimate the mechanical parameters accurately, both of them have poor robustness. In [11]-[12], active disturbance rejection adaptive control (ADRC) scheme is adopted for motion control of servo systems. The control strategy can perform well, but its complexity in structure makes it not easy to implement. Moreover, it is subjected to both parametric uncertainties and uncertain nonlinearities. In [13], a full-order Luenberger observer is adopted for system parameter identification algorithm, where the inertia is estimated by observing the position error. However, the performance of the proposed full-order observer is affected by the initial value of the moment of inertia, and in the worst case, the system becomes unstable [13]. Li Niu et al. [14] utilized a reduced-order Luenberger observer to estimate the load torque and consequently the inertia information. A common problem in [13] and [14] is that there is an estimation error from the Luenberger observer no matter whether the inertia information is accurate or not. Reference [15-17] proposed algorithms based on the extended Kalman filter (EKF), where the mechanical parameters are treated as system variables and can be estimated directly by EKF. However, the recursive least square algorithm used to solve the least squares estimation upon convergence depends much on the initial conditions and requires a long estimation time with a special trajectory of reference velocity during the identification. Therefore, the application of these methods [15-17] in real systems is limited.

Compared to the above-mentioned methods, sliding mode observers (SMO) has the attractive advantages of robustness against disturbances, low sensitivity to the system parameter variations, fast response and easy implementation [18-20]. Therefore, many SMO-based parameter identification methods have been proposed. References [21-22] introduced SMO-based control schemes to handle the time-varying parameters and disturbances of PMSM drive systems. References [23-25] extended the SMO by including the errors/disturbances of the mechanical parameters in the state space equations for estimating the mechanical parameters and system disturbances of the PMSM drive system. However, in

This work is supported by Zhejiang Provincial Natural Science Foundation of China (Grant No.LY18E070006, LY18E050016) and National Natural Science Foundation of China(Grant No.51307151, 51677172). (Corresponding author: Kaiyuan Lu.)

W. Lu, Z. Zhang, D. Wu, K. Ji and L. Guo are with the Faculty of Mechanical Engineering and Automation, Zhejiang Sci-Tech University, 928 Second Avenue, Xiasha Higher Education Zone,Hangzhou, 310018, China (e-mail: luwenqi@zstu.edu.cn; zzyymx712@163.com; wudi4761@163.com; jkh@zstu.edu.cn; lguo@zstu.eu.cn).

D. Wang and K. Lu are with the Department of Energy Technology, Aalborg University, DK-9220 Aalborg, Denmark (e-mail:klu@et.aau.dk; dwa@et.aau.dk).

This article has been accepted for publication in a future issue of this journal, but has not been fully edited. Content may change prior to final publication. Citation information: DOI 10.1109/TPEL.2018.2881217, IEEE Transactions on Power Electronics

aforementioned conventional SMOs, the sign function will cause a high frequency chattering/buffeting problem [25], which could create system oscillation, performance degradation, or even system instability [25]. A compromising solution is to add a low-pass filter (LPF) to obtain the useful information of the estimated parameters [26]. Unfortunately, the introduction of the LPF will lead to phase delay, which affect the estimation accuracy and the performance of the drive system. Thus, proper compensation is required to mitigate the influence of the LPF, especially when estimating AC signals where continuous phase delay exhibits [26].

In this paper, the mathematical model of the conventional load torque identification (LTID) SMO is derived, analyzed and further developed. A new LTID-SMO with adaptive compensation algorithm is proposed to mitigate the chattering/buffeting problem of conventional SMOs, as well as improving the estimation accuracy. The proposed SMO is analyzed theoretically and verified by experimental tests.

II. CONVENTIONAL LTID-SMO

The mathematical model of a conventional LTID-SMO of a PMSM drive system is described in this section by following the sliding mode variable structure control theory [23-25].

The voltage equation of the PMSM in the dq reference frame can be expressed as:

$$\begin{cases} u_d = Ri_d + pL_d i_d - \omega_e L_q i_q \\ u_q = Ri_q + pL_q i_q + \omega_e (L_d i_d + \psi_f) \end{cases} \tag{1}$$

where R is the stator resistance; u_d, u_q, i_d, i_q, L_d, and L_q are stator d- and q-axes voltages, currents, and inductances, respectively; ψ_f is the rotor permanent magnet flux-linkage; ω_e is the motor electrical angular velocity; and p represents the differential operation.

The torque equation of the PMSM is:

$$T_e = \frac{3}{2} p_n \left[\psi_f i_q - (L_q - L_d) i_d i_q \right] \tag{2}$$

where p_n is the number of machine pole-pairs; and T_e is the electromagnetic torque.

The motion equation of the PMSM is:

$$J \frac{d\omega_r}{dt} = T_e - B\omega_r - T_L \tag{3}$$

where J is the moment of inertia; T_L is the load torque; B is the viscous friction coefficient; and ω_r is the motor mechanical angular velocity.

By substituting (2) into (3), it can be obtained that:

$$\frac{d\omega_e}{dt} = \frac{1.5 p_n^2}{J} [\psi_f i_q + (L_d - L_q) i_d i_q] - \frac{p_n}{J} T_L - \frac{B}{J} \omega_e \tag{4}$$

The speed estimation formula of the conventional LTID-SMO can be expressed as follow [25]:

$$\frac{d\hat{\omega}_e}{dt} = \frac{1.5 p_n^2}{J} [\psi_f i_q + (L_d - L_q) i_d i_q] - \frac{B}{J} \hat{\omega}_e - Z_s \tag{5}$$

where $\hat{\omega}_e$ is the estimated speed, $Z_s = k \cdot \text{sign}(\hat{\omega}_e - \omega_e)$ is the switching signal defined by a sign function, and k is the sliding mode gain.

Defining the speed estimation error as $\tilde{\omega}_e = \hat{\omega}_e - \omega_e$, it can be obtained by subtracting (4) from (5) that:

$$\frac{d\tilde{\omega}_e}{dt} = \frac{p_n}{J} T_L - \frac{B}{J} \tilde{\omega}_e - Z_s \tag{6}$$

The sliding surface is defined as:

$$S(x) = \tilde{\omega}_e = \hat{\omega}_e - \omega_e \tag{7}$$

According to the sliding mode control (SMC) theory, it satisfies $S_s = \dot{S}_s = 0$ when the system enters the steady state and sliding around the sliding mode surface. Thus, the load torque can be estimated as:

$$\hat{T}_L = \frac{J}{p_n} Z_s \tag{8}$$

Due to the discontinuity of the control function in SMC, the estimated load torque $\hat{T}_L$ obtained by (8) contains high frequency noise, i.e.:

$$\hat{T}_L = T_L + \Delta u_s \tag{9}$$

where Δu_s is the high frequency noise caused by the discontinuous switching operations of the sign function, which can result in system chattering. Therefore, in order to obtain an effective LTID value without chattering, a LPF is needed to filter out the high order harmonics. Then, the estimated load torque can be expressed as:

$$\hat{T}_L = \frac{J}{p_n} Z_s \cdot \frac{\omega_c}{s + \omega_c} \tag{10}$$

where ω_c is the cut-off frequency of the LPF. However, the involvement of the LPF will inevitably introduce system error and delay during the load torque transient. This error and delay should be compensated properly in order to achieve satisfactory performance. Based on the above principle, the principle block diagram of the traditional LTID-SMO when used for load torque estimation can be obtained as shown in Fig.1.

This article has been accepted for publication in a future issue of this journal, but has not been fully edited. Content may change prior to final publication. Citation information: DOI 10.1109/TPEL.2018.2881217, IEEE Transactions on Power Electronics

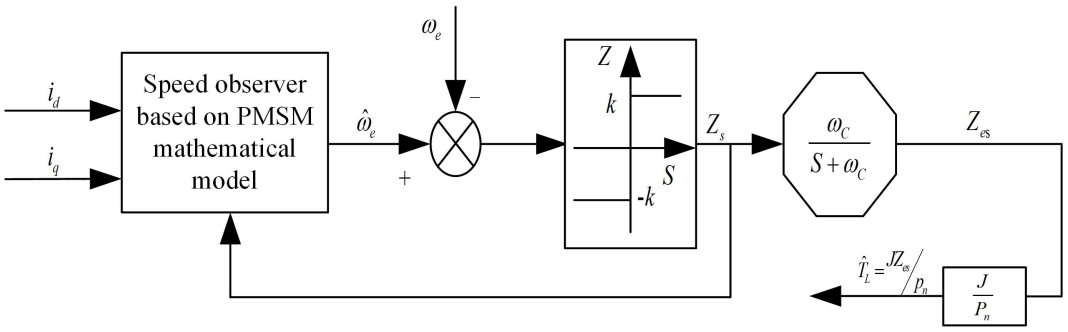

Fig. 1. The principle block diagram of the conventional LTID-SMO.

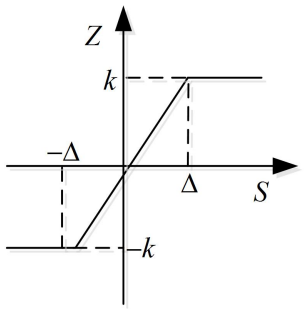

Fig. 2. The saturation function.

III. PROPOSED LTID-SMO

The conventional LTID-SMO shown in Fig. 1 mainly consists of a mathematical model of a speed observer, a sign function, a LPF, and the load torque estimator. Since discontinuous sign function is used to adjust the load torque indicating signal, it results in system high frequency chattering/buffeting, which can degrade the system performance (e.g. increased current and torque ripples as well as energy losses) or even cause system oscillation/instability. The introduction of the LPF can help to mitigate the buffeting problem at steady state conditions, but will affect the accuracy of the LTID during transient conditions. In order to solve these problems, this paper proposes an improved LTID-SMO by replacing the sign function with a saturation function and improving the LTID algorithm, which are described and analyzed in this section.

A. Switching function modification

The fundamental reason of the buffeting is the discontinuity of the switching signal around the sliding surface due to the characteristics of the sign function. Thus, if replacing the discontinuous sign switching operation with continuous function around the sliding surface, the variation of the switching signal Z_s can be limited, so that a smoothened output can be obtained and the high frequency buffeting can be effectively mitigated. In this paper, a simple saturation function with linear changes within the $\pm\Delta$ region is adopted as defined in (11) and shown in Fig. 2.

$$Z_{s1}(n)=\begin{cases} k, & \hat{\omega}_e-\omega_e>\Delta \\ \dfrac{k}{\Delta}\left[\hat{\omega}_e-\omega_e\right], & -\Delta<\hat{\omega}_e-\omega_e<\Delta \\ -k, & \hat{\omega}_e-\omega_e<-\Delta \end{cases} \tag{11}$$

B. Analysis of modified LTID algorithm

Besides replacing the sign function with the saturation function, the LTID algorithm is further improved by introducing an extra component to represent the average estimated load torque and involving it in the speed observer. The motion state equation of the proposed LTID-SMO can be expressed as:

$$\frac{d\hat{\omega}_e}{dt}=\frac{1.5p_n^2}{J}[\psi_f i_q+(L_d-L_q)i_d i_q]-lZ_{es}-\frac{B}{J}\hat{\omega}_e-Z_{s1} \tag{12}$$

where $Z_{s1}=k\cdot sat(\hat{\omega}_e-\omega_e)$ is the load torque indicating signal determined by the saturation function, Z_{es} is the large signal of Z_{s1}, and l is the feedback gain of Z_{es}. Z_{es} can be obtained through a LPF:

$$Z_{es}=Z_{s1}\cdot\omega_c/(s+\omega_c) \tag{13}$$

It can be obtained by subtracting (4) from (12) that:

$$\frac{d\tilde{\omega}_e}{dt}=\frac{p_n}{J}T_L-lZ_{es}-\frac{B}{J}\tilde{\omega}_e-Z_{s1} \tag{14}$$

The sliding surface is defined as (7), and the load torque can be estimated as:

$$\hat{T}_L=\frac{J}{p_n}(lZ_{es}+Z_{s1}) \tag{15}$$

It can be seen from (15) that the LTID method based on the improved SMO consists of two parts: $J(lZ_{es})/p_n$ and $J(Z_{s1})/p_n$ respectively. $J(lZ_{es})/p_n$ contains mainly the low

This article has been accepted for publication in a future issue of this journal, but has not been fully edited. Content may change prior to final publication. Citation information: DOI 10.1109/TPEL.2018.2881217, IEEE Transactions on Power Electronics

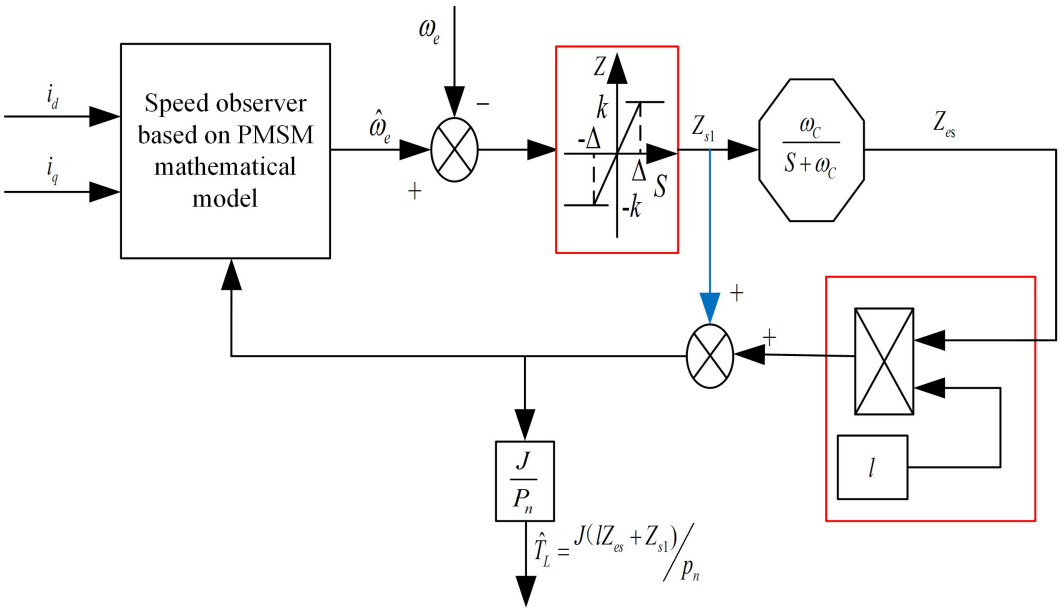

Fig. 3. The block diagram of the proposed LTID-SMO.

frequency component of the estimated torque, while $J(Z_{s1})/p_n$ contains mainly the harmonic component caused by the load torque indicating signal Z_{s1}. At steady state condition with constant load, it can be expressed that:

$$Z_{es} = \langle Z_{s1} \rangle = \frac{p_n}{J(1+l)} T_L \tag{16}$$

It should be noted that the output of the saturation function is limited to k, i.e. $Z_{es} = \langle Z_{s1} \rangle \le k$. Thus, the value of the gain factors k and l should satisfy the following condition:

$$k \ge \frac{p_n}{J(1+l)} T_L \tag{17}$$

Compared with the conventional LTID algorithm, the improved LTID algorithm can limit the harmonic content by adjusting the feedback gain l. Thus, the buffeting of the estimated torque is reduced. Moreover, since the load torque indicating signal, which can represent the load torque change without extra delay, is directly involved in the estimated load torque (as the blue arrow indicated in Fig. 3), the estimation delay caused by the LPF can be compensated to a large extent. By adjusting the parameters Δ, k of the saturation function and the feedback gain l of the Z_{es} together, satisfactory performance can be achieved during the transients with balanced system chattering mitigation and response speed. The block diagram of the improved LTID-SMO can be seen in Fig. 3.

IV. Stability Analysis of Proposed LTID-SMO

The modified SMO described in (14) is used for stability analysis. When $S > \Delta$, the output signal of the saturation function is constant k (i.e. $Z_{s1} = k$), so as the output of the LPF (i.e. $Z_{es} = k$). Similarly, for condition $S < -\Delta$, it has $Z_{s1} = Z_{es} = -k$. When the SMO is operating around the sliding surface (i.e. $-\Delta < S < \Delta$), supposing the cut-off frequency of the LPF is high and the effective signal of S (i.e. not including the noise) is not affected, it has $Z_{s1} = Z_{es} = S \cdot k/\Delta$. Then, (14) can be re-written as:

$$\frac{dS}{dt} + \frac{B}{J} S - \frac{p_n}{J} T_L = \begin{cases} -k(1+l), & S > \Delta \\ -\frac{k}{\Delta} S(1+l), & -\Delta < S < \Delta \\ k(1+l), & S < -\Delta \end{cases} \tag{18}$$

where the sliding surface S is the speed error $\tilde{\omega}_e$ as defined in (7). According to the Routh-Hurwitz stability criterion, when $S > \Delta$ or $S < -\Delta$, the system is stable if $B/J > 0$, which is always true; when $-\Delta < S < \Delta$, the system is stable if $B/J + (1+l) \cdot k/\Delta > 0$, which is always hold as well, since all the parameters have positive values. The larger the coefficient $B/J + (1+l) \cdot k/\Delta$ value is, the larger the system damping factor becomes, and the shorter the system transient is.

If taking the influence of the LPF into consideration when the speed error varies around the sliding surface, i.e. $-\Delta < S < \Delta$, the system equation in the frequency domain can be expressed as:

This article has been accepted for publication in a future issue of this journal, but has not been fully edited. Content may change prior to final publication. Citation information: DOI 10.1109/TPEL.2018.2881217, IEEE Transactions on Power Electronics

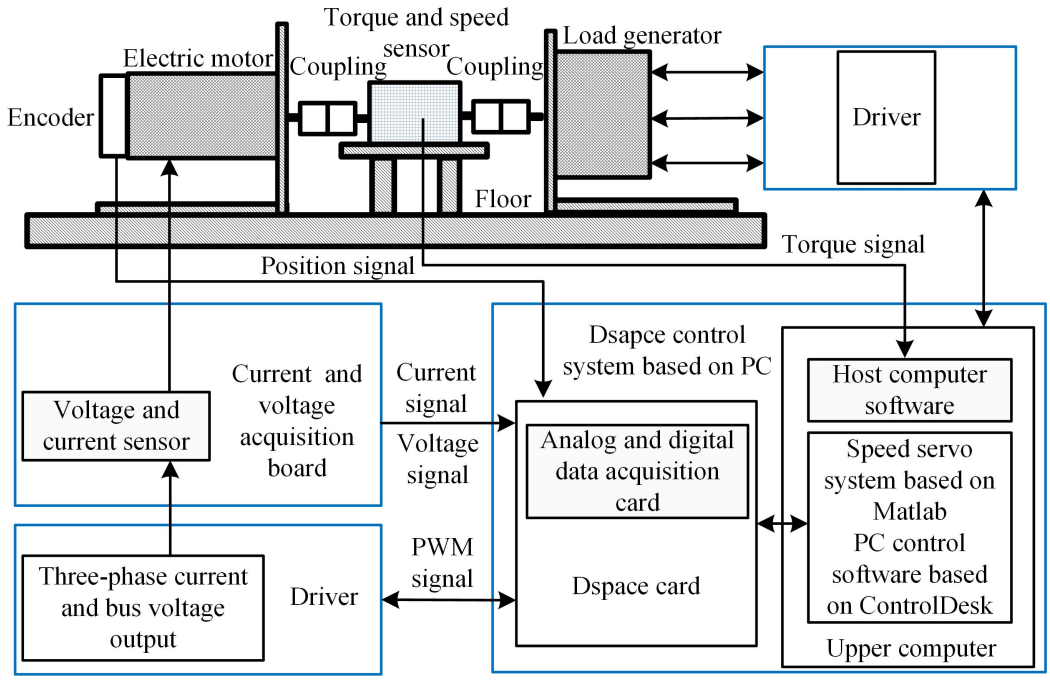

Fig. 4. The block diagram of the dSPACE based motor drive test platform.

$$s\tilde{\omega}_e+\frac{B}{J}\tilde{\omega}_e-\frac{p_n}{J}T_L=-\frac{k}{\Delta}\tilde{\omega}_e\left(1+l\cdot\frac{\omega_c}{s+\omega_c}\right) \tag{19}$$

where s is the complex variable of Laplace transform, and $\tilde{\omega}_e$ is used to replace s to avoid possible confusion. By re-writing (18), it can be obtained that:

$$s^2\tilde{\omega}_e+\left(\omega_c+\frac{B}{J}+\frac{k}{\Delta}\right)s\tilde{\omega}_e+\omega_c\left(\frac{B}{J}+\frac{k}{\Delta}(1+l)\right)\tilde{\omega}_e=\frac{p_n}{J}\left(\dot{T}_L+\omega_c T_L\right) \tag{20}$$

where $\dot{T}_L$ is the time derivative of T_L. According to Routh-Hurwitz stability criterion, the system is stable if $\left(\omega_c+\frac{B}{J}+\frac{k}{\Delta}\right)>0$ and $\omega_c\left(\frac{B}{J}+\frac{k}{\Delta}(1+l)\right)>0$, which is always true for the proposed LTID-SMO. It can be seen from the above analysis that the proposed LTID-SMO is always stable, which is a big advantage.

Moreover, it can be observed from (18) that when $S>\Delta$ and $S<-\Delta$, the characteristic value is $-\frac{B}{J}$, which is the same as conventional SMO. When $-\Delta<S<\Delta$, the characteristic value becomes $-\frac{B}{J}-\frac{k}{\Delta}$. An extra part is introduced, which increases the damping factor and fastens the convergence rate of the speed error. Therefore, the introduction of the saturation function not only reduces the system chattering, but also improves its convergence rate.

TABLE I
THE KEY PARAMETERS OF THE MOTOR TEST PLATFORM

Electric motor[PMSM]parameters		Key equipment parameter	
Rated speed [r/min]	2000	Load generator[PMSM]	SIEMENS 1FK7080
Rated torque [N.m]	6	Torque speed sensor	DR-3000
Number of pole-pairs	4	dSpace platform	DS1103
Resistance [Ω]	0.68		
Q-axis and d-axis inductor [mH]	0.0055		
Total moment of inertia [kg.m^2]	0.01482		
Rated voltage [V]	380		

V. EXPERIMENTAL VERIFICATION

In order to verify the advantages of the proposed scheme, a speed servo system with a PMSM drive is built as illustrated in Fig. 4 and 5, where dSPACE is used to implement the control algorithms with both conventional and proposed LTID-SMOs for comparison. The parameters of the key devices are shown in Table I. The control scheme of the speed servo system is shown in Fig. 6, where field-oriented control (FOC) with speed control loop is enhanced with LTID-SMO.

This article has been accepted for publication in a future issue of this journal, but has not been fully edited. Content may change prior to final publication. Citation information: DOI 10.1109/TPEL.2018.2881217, IEEE Transactions on Power Electronics

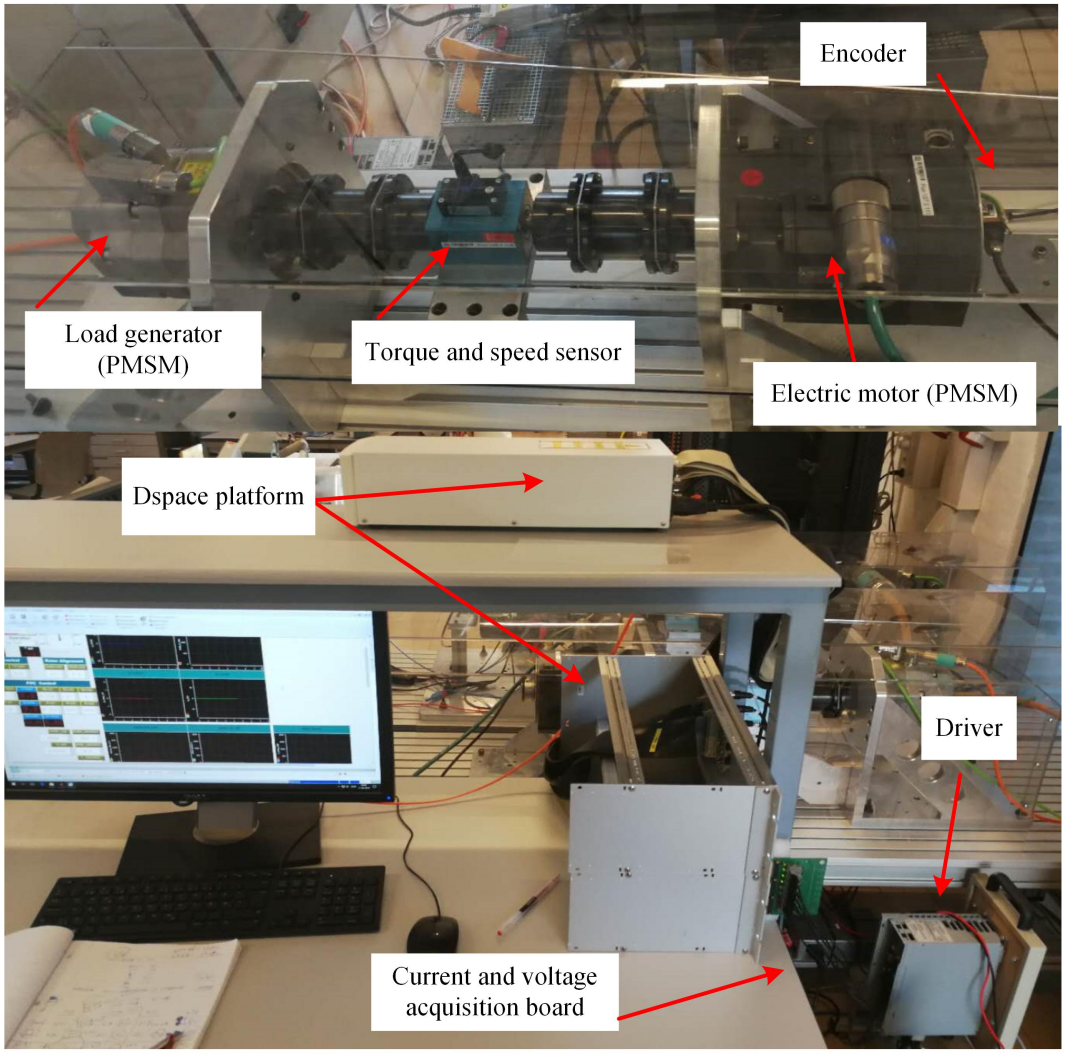

Fig. 5. The motor drive test setup.

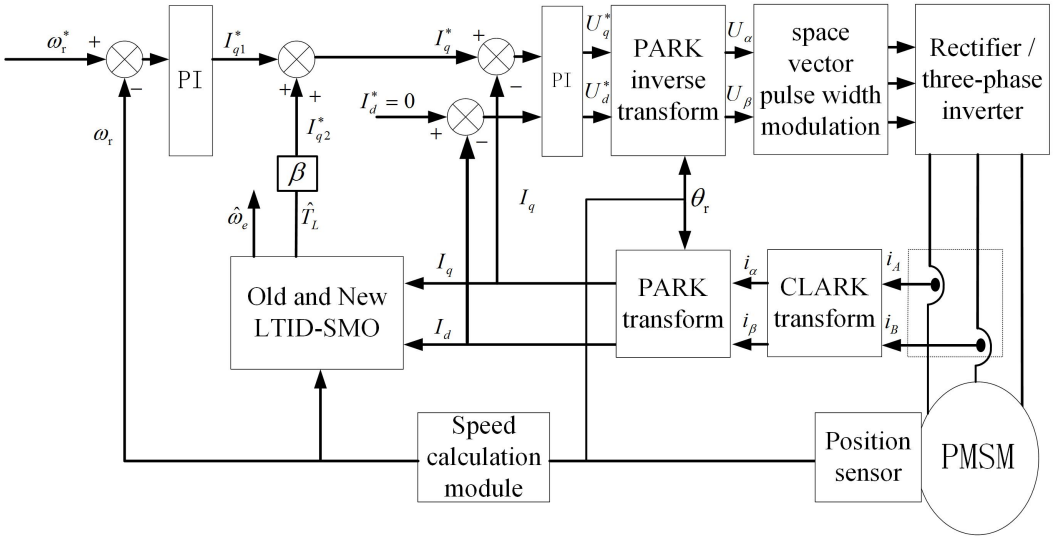

Fig. 6. The control scheme of the speed servo drive system with LTID-SMO.

This article has been accepted for publication in a future issue of this journal, but has not been fully edited. Content may change prior to final publication. Citation information: DOI 10.1109/TPEL.2018.2881217, IEEE Transactions on Power Electronics

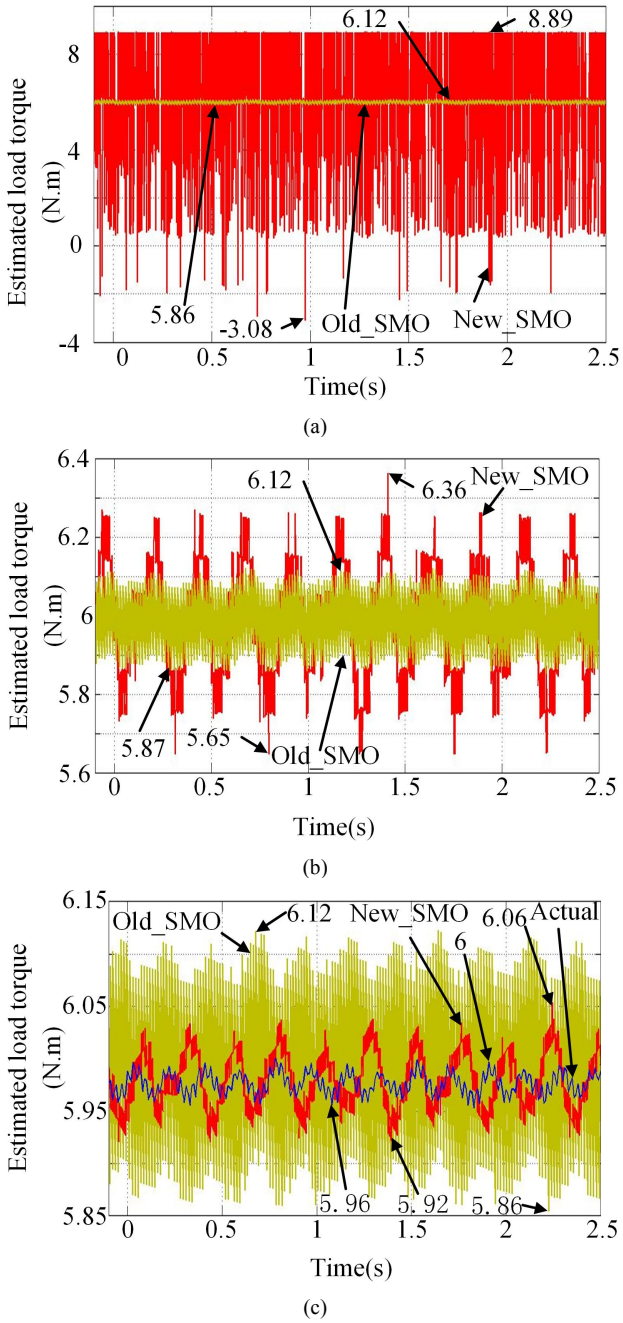

Fig. 7. The performance of using a saturation function to replace the sign function, when motor operates at 1000 r/min full load torque (6 N.m) condition, and l =0. (a) the estimated load torque when Δ =0.1. (b) the estimated load torque when Δ =5. (c) the estimated load torque when Δ =30.

A. Performance of proposed LTID-SMO

According to the previous analysis, the proposed LTID-SMO has two main modifications compared with the conventional LTID-SMO: i) replacing the sign function with a saturation function; ii) improving the LTID algorithm by introducing an extra component to represent the average estimated load torque and involving it in the speed observer. It is worth to point out that i) when the boundary layer of the saturation function Δ is set to zero, the saturation function is degraded to the sign function; ii) when the feedback gain l is set to zero, the proposed LTID-SMO is degraded to the conventional LTID-SMO.

The effectiveness of using a saturation function instead of the sign function is investigated first with the following test conditions: the motor operates at 1000 r/min with full load torque (6 N.m); the values of the sliding mode gain k of both the saturation and sign functions are the same; the feedback gain l is set to zero (i.e. without involving of improved LTID algorithm). The test performance with different values of Δ are shown in Fig. 7, where the waveforms obtained by the proposed LTID-SMO are drawn in red line and marked with "New_SMO"), the waveforms obtained by the conventional LTID-SMO are drawn in yellow line and marked with "Old_SMO", and the waveforms obtained by the torque/speed sensor are drawn in blue line and marked with "Actual". The above notations are followed for the rest of the figures in this section.

Fig. 7 (a) gives the estimated load torque waveforms when Δ =0.1, where the saturation function is close to the sign function. It can be seen that the estimated load torque waveform obtained by the proposed LTID-SMO has much larger ripples than that of the conventional LTID-SMO. This is because that the proposed LTID-SMO does not contain any LPF when l =0, while a LPF is used to smoothen the estimated load torque in the conventional LTID-SMO. Fig. 7 (b) and (c) gives the estimated load torque waveforms when Δ =5 and Δ =30 respectively (with l =0). It can be observed that the buffeting of the estimated load torque obtained by the proposed LTID-SMO reduces as Δ increases. When Δ =30, the estimated load torque obtained by the proposed LTID-SMO is varying between 5.92-6.06 N.m, which is less than that obtained by the conventional LTID-SMO and is close to the actual load torque. To further improve its performance, the feedback gain l is then introduced to the LTID algorithm and is tested.

To examine the improved LTID algorithm with feedback gain l, investigations are done with the following test conditions: the motor operates at 1000 r/min with full load torque (6 N.m); the values of the sliding mode gain k of both the saturation and sign functions are the same; and Δ is set to 30. The test performance with different values of l are shown in Fig. 8. It can be observed from Fig. 8 (a) and (b) that the ripples of the estimated load torque obtained by the proposed LTID-SMO becomes even small than the actual load torque, and the increasing of l will not further reduce the torque ripple.

Therefore, compared with the conventional LTID-SMO, the proposed LTID-SMO can effectively reduce the buffeting of the estimated load torque without sacrificing other performance by adjusting the boundary layer Δ and the feedback gain l synergistically.

B. LTID-SMO performance comparison

In order to verify the superiority of the proposed LTID-SMO, the performance comparison with the conventional LTID-SMO is carried out on two operating states when l =5, Δ =20, k =500: 1) constant speed with constant load, and 2) constant speed with sudden load change, respectively.

This article has been accepted for publication in a future issue of this journal, but has not been fully edited. Content may change prior to final publication. Citation information: DOI 10.1109/TPEL.2018.2881217, IEEE Transactions on Power Electronics

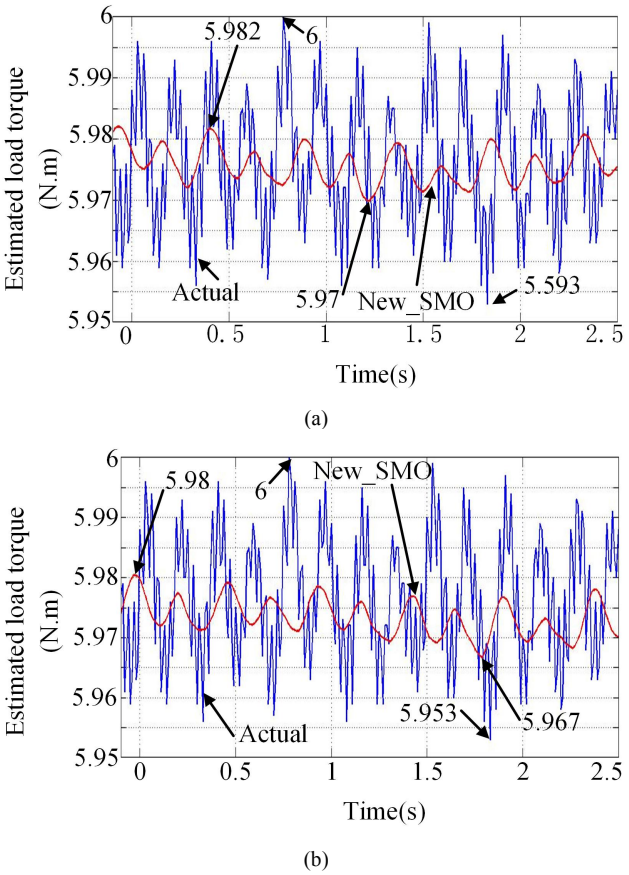

Fig. 8. The performance of involving improved LTID algorithm with feedback gain, when motor operates at 1000 r/min full load torque (6 N.m) condition, and Δ =30. (a) the estimated load torque when l =5. (b) the estimated load torque when l =15.

1) Constant speed with constant load

The performance comparison between the conventional and proposed observers is carried out at a given constant speed of 500 r/min and 2000 r/min with a given constant load torque of half- and full-load respectively as shown in Fig. 9. It can be seen from Fig. 9 (a) that compared with the average load torque of 2.98 N.m at 500 r/min, the maximum ripple of the actual load torque, estimated load torque obtained by the conventional and proposed LTID-SMOs are 0.26%, 2.7% and 0.97%, respectively. Similarly, the performance comparison of other operation conditions can be found and summarized in Table II.

Therefore, it can be seen from the experimental results that the estimated load torque value obtained from the proposed LTID-SMO, compared with that from the conventional LTID-SMO, has smaller buffeting at constant speed and load conditions.

2) Constant speed with sudden load change

The performance comparison between the conventional and proposed observers is then carried out at a given constant speed of 500 r/min and 2000 r/min with a given sudden load change of half- and full-load torque respectively as shown in Fig. 10.

It can be seen from Fig. 10 (a) that a sudden load and unload of 3.05 N.m is applied to the PMSM drive at 0.5s and 3.7s respectively. It can be observed that it takes 1s for the

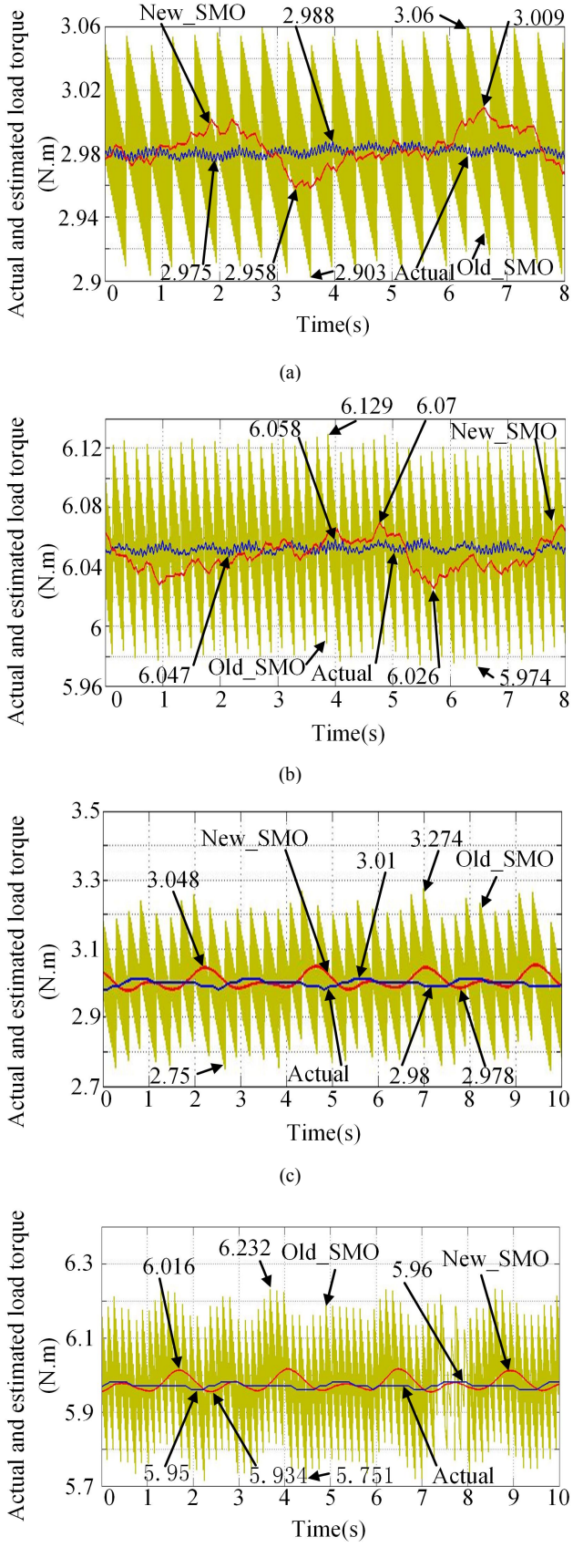

Fig. 9. Load torque estimation performance comparison. (a) 500 r/min with half load torque (3 N.m). (b) 500 r/min with full load torque (6 N.m). (c) 2000 r/min with half load torque. (d) 2000 r/min with full load torque.

This article has been accepted for publication in a future issue of this journal, but has not been fully edited. Content may change prior to final publication. Citation information: DOI 10.1109/TPEL.2018.2881217, IEEE Transactions on Power Electronics

TABLE II
PERFORMANCE COMPARISON AT CONSTANT SPEED WITH CONSTANT LOAD CONDITIONS

Operating condition	Average torque [N.m]	Maximum torque ripple [100%]		
		Actual	Conventional observer	Proposed observer
500 r/min, 3 N.m	2.98	0.26%	2.7%	0.97%
500 r/min, 6 N.m	6.05	0.13%	1.3%	0.4%
2000 r/min, 3 N.m	3.0	0.33%	9.1%	1.6%
2000 r/min, 6 N.m	5.97	0.17%	4.4%	0.8%

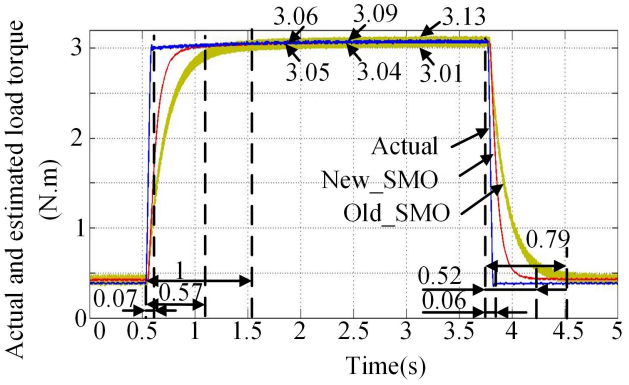

(a)

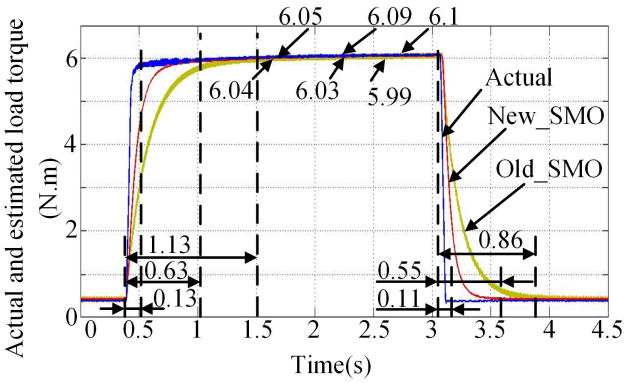

(b)

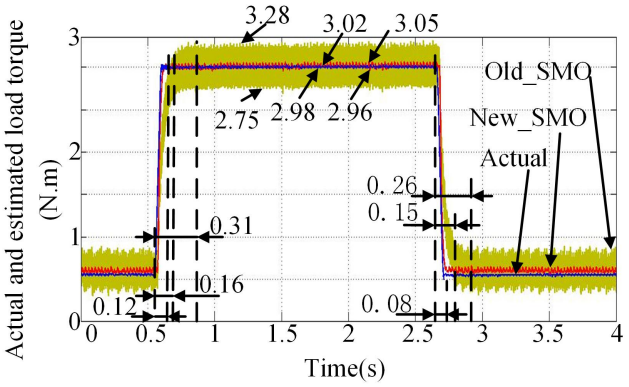

(c)

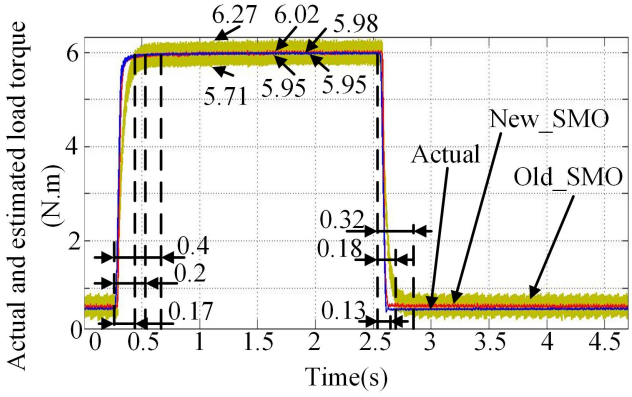

(d)

Fig. 10. Load torque estimation performance comparison. (a) 500 r/min with half load torque step change. (b) 500 r/min with full load torque step change. (c) 2000 r/min with half load torque step change. (d) 2000 r/min with full load torque step change.

TABLE III
PERFORMANCE COMPARISON AT CONSTANT SPEED WITH SUDDEN LOAD CHANGE CONDITIONS

Operating condition	Step load on, response time [s]		Step load off, response time [s]	
	Conventional	Proposed	Conventional	Proposed
500 r/min, 3 N.m	1	0.57	0.79	0.52
500 r/min, 6 N.m	1.13	0.63	0.86	0.55
2000 r/min, 3 N.m	0.31	0.16	0.26	0.15
2000 r/min, 6 N.m	0.4	0.2	0.32	0.18

conventional LTID-SMO to reach an average torque of 3.05N.m when there is a sudden load, while it only takes 0.57s for the proposed LTID-SMO to reach the actual load torque change. Table III summarizes the performance comparison at this operating state.

Therefore, it can be seen from the experimental results that the proposed LTID-SMO, compared with the conventional LTID-SMO, has the advantages of smaller buffeting and faster dynamic response under the same condition of constant speed with step load change.

C. Driving performance test of the speed servo system

To further verify the advantages of the proposed LTID-SMO, the speed transients of the speed servo system during the sudden load change conditions are examined experimentally.

Fig. 11 shows the experiment results at a given speed of 500 r/min with full load torque sudden changes. It can be observed that the speed of the servo system without the proposed LTID-SMO falls to 458.2 r/min and then returns to 500 r/min after 2.8s, when there is a sudden load change with full load torque. The speed of the servo system with proposed LTID-SMO falls to 461.7 r/min, and then returns to 500 r/min after 0.5s under the same condition. The recovery time is

This article has been accepted for publication in a future issue of this journal, but has not been fully edited. Content may change prior to final publication. Citation information: DOI 10.1109/TPEL.2018.2881217, IEEE Transactions on Power Electronics

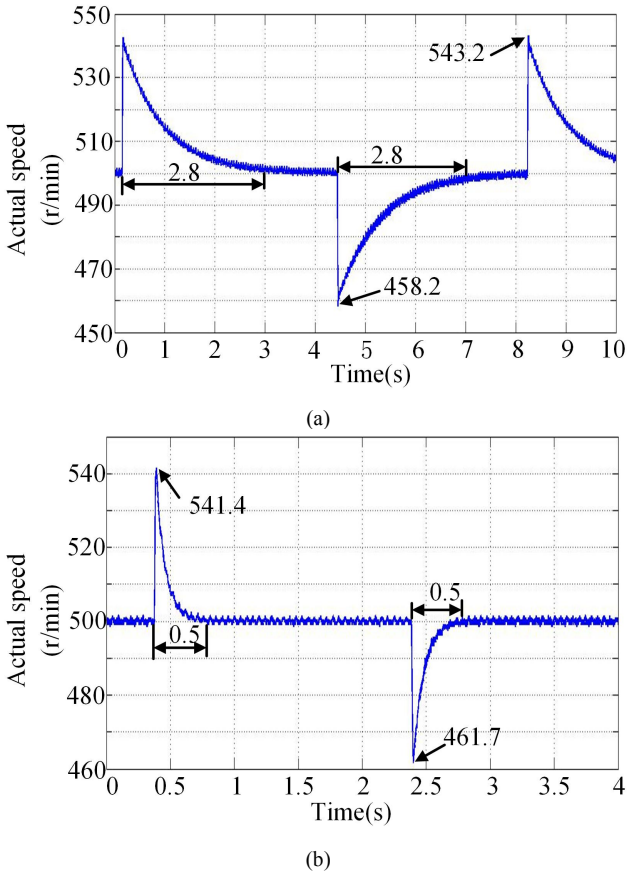

Fig. 11. The actual speed waveforms during the sudden full load torque changes at 500r/min. (a) without proposed LTID-SMO. (b) with proposed LTID-SMO.

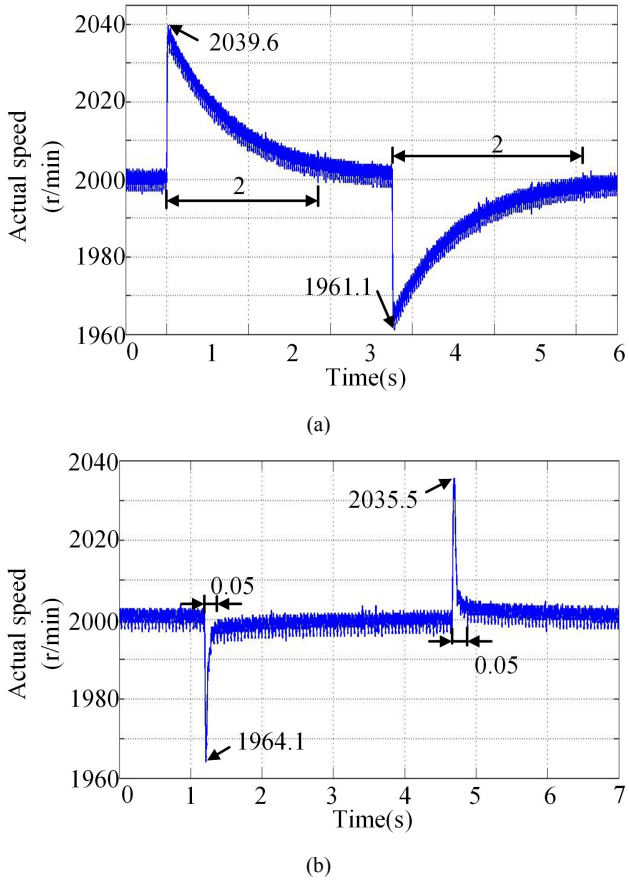

Fig. 12. The actual speed waveforms during the sudden full load torque changes at 2000r/min. (a) without proposed LTID-SMO. (b) with proposed LTID-SMO.

greatly reduced by the introducing of the proposed LTID-SMO. Similarly for sudden unload condition, the introducing of the proposed LTID-SMO can shorten the recovery time from 2.8s to 0.5s. Fig. 12 shows the experiment results at a given speed of 2000 r/min with full load sudden changes. It can be seen that the recovery time under sudden load change conditions of the speed servo system with the proposed LTID-SMO are reduced from 2s to 0.05s. Therefore, it can be concluded that introducing of the proposed LTID-SMO can greatly improve the speed regulation performance of the servo drive system against sudden load torque changes.

VI. Conclusion

In this paper, the high frequency chattering problems of the existing LTID-SMO are analyzed. The model of the existing SMOs is improved by replacing the sign function with a saturation function and introducing a new LTID algorithm with an extra feedback loop. The mathematical model of the improved LTID-SMO is built, and its stability is analyzed. The proposed LTID-SMO is verified by experiments. It is shown by experiments that the proposed LTID-SMO has much smaller buffeting and much faster dynamic response during load torque transient. Moreover, the introducing of the proposed LTID-SMO in the speed servo system can help to shorten the recovery time greatly in processes with sudden load changes.

References

[1] W.Lu, K.JI, "Double Position Servo Synchronous Drive System Based on Cross-Coupling Integrated Feedforward Control for Broacher," *Chinese Journal of Mechanical Engineering*, vol.30 , no. 2, pp. 272-285, Jan. 2017.

[2] W. Lu, X. Hu, W. Shi, L.Lin, X.Deng, " The control strategy of synchronous driving disturbance compensation algorithm based on dual servo broaching machine main slide board, " *Journal of Mechanical Engineering*, vol. 49, no. 21, pp. 31-37, Nov. 2013.

[3] K. Ohishi, R. Furusawa, "Actuators for Motion Control: Fine Control for Electric Injection Molding Machines, " *IEEE Industrial Electronics Magazine*, vol. 6, no. 1, pp. 4-13, Mar. 2012.

[4] Y. Ohba, M. Sazawa, K. Ohishi, T. Asai, K. Majima, Y. Yoshzawa, Y. Yoshzawa, K. Kageyama, "Sensorless Force Control for Injection Molding Machine Using Reaction Torque Observer Considering Torsion Phenomenon, " *IEEE Transactions on Industrial Electronics*, vol. 56, no. 8, pp. 2955-2960, Jun. 2009.

[5] W. Lu, Y. Hu, H. Jin, X.Hu, "The parameters of the crank servo pressure motor force system driven by permanent magnet synchronous motor, " *Transactions of China Electrotechnical Society*, vol. 29, no. 1, pp. 91-97, Jan. 2014.

[6] H. Cheng, L. Pei, "Experimental study on a hybrid-driven servo press using iterative learning control," *International Journal of Machine Tools and Manufacture*, vol. 48, no. 2, pp. 209-219, Feb. 2008.

[7] J. Linares-Flores, C. García-Rodríguez, H. Sira-Ramírez, O. D. Ramírez-Cárdenas, " Robust Backstepping Tracking Controller for Low-Speed PMSM Positioning System: Design, Analysis, and Implementation," *IEEE Transactions On Industrial Informatics*, vol. 11, no. 5, pp. 1131-1141, Oct. 2015.

[8] Y. Mei, K. Sun,Y. Shi, "A 2-D fuzzy logic based MRAS scheme for sensorless control of interior permanent magnet synchronous motor

drives with cyclic fluctuating loads, " *Chinese Journal of Electrical Engineering*, vol. 1, no. 1, pp. 85-91, Dec. 2015.
[9] W. Chen, J. Yang, L. Guo, "Disturbance-Observer-Based Control and Related Methods An Overview, " *IEEE Transactions on Industrial Electronics*, Vol. 63, no. 2, pp. 1083-1095, Feb. 2016.
[10] X. Zhang, B. Hou, Y. Mei, " Deadbeat Predictive Current Control of Permanent-Magnet Synchronous Motors with Stator Current and Disturbance Observer, " *IEEE Transactions on Power Electronics*,vol. 32, no. 5, pp. 3818-3834, May. 2017.
[11] J. Yao, W. Deng, " Active Disturbance Rejection Adaptive Control of Hydraulic Servo Systems," *IEEE Transactions on Industrial Electronics*, Vol.64, no. 10, pp. 8023-8032, Oct. 2017.
[12] B. Du, S. Wu, S. Han, S.Cui, "Application of Linear Active Disturbance Rejection Controller for Sensorless Control of Internal Permanent-Magnet Synchronous Motor, " *IEEE Transactions on Industrial Electronic*s, vol. 63, no. 5, pp. 3019-3027, May. 2016.
[13] C.M. Verrelli, A. Savoia, M. Mengoni, " On-Line Identification of Winding Resistances and Load Torque in Induction Machines, " *IEEE Transactions On Control Systems Techology*, vol. 22, no. 4, pp. 2395-2403, Jul. 2014.
[14] L. Niu, D. Xu, M. Yang, "On-line Inertia Identification Algorithm for PI Parameters Optimization in Speed Loop," *IEEE Transactions On Power Electronics*, vol. 30, no. 2, pp. 849-859, Feb. 2015.
[15] N. Hoffmann, F. W. Fuchs, "Minimal invasive equivalent grid impedance estimation in inductive-resistive power networks using extended Kalman filter," *IEEE Transaction Power Electron*, vol. 29, no. 2, pp. 631-641, Feb. 2014.
[16] G. Rigatos, P. Siano, N. Zervos, C.Cecati, " Control and Disturbances Compensation for Doubly Fed Induction Generators Using the Derivative-Free Nonlinear Kalman Filter," *IEEE transactions on Power Electronics*, vol. 30, no. 10, pp. 5532-5547, Oct.2015.
[17] T. Shi, Z. Wang, C. Xia, " Speed Measurement Error Suppression for PMSM Control System Using Self-Adaption Kalman Observer," *IEEE Transactions on Industrial Electronics*, Vol. 62, no. 5, pp. 2753-2763, May. 2015.
[18] T. Bernardes, V. F. Montagner, H. A. Gründling, H.Pinheiro., "Discrete-Time Sliding Mode Observer for Sensorless Vector Control of Permanent Magnet Synchronous Machine, " *IEEE Transactions on Industrial Electronics*, vol. 61, no. 4, pp. 1679-1691, Apr. 2014.
[19] Z. Qiao, T. Shi,, Y. Wang, Y.Yan, C.Xia, X.He, " New Sliding-Mode observer for Position Sensorless Control of Permanent-Magnet Synchronous Motor, " *IEEE Transactions on Industrial Electronics*, vol.60, no. 2, pp. 710-719, Feb. 2013.
[20] Y. Fan, L. Zhang, M. Cheng, " Sensorless SVPWM-FADTC of a New Flux-Modulated Permanent-Magnet Wheel Motor Based on a Wide-Speed Sliding Mode Observer," *IEEE Transactions on Industrial Eletronics*, vol. 62, no. 5, pp. 3143-3151, May. 2015.
[21] V. Q. Leu, H. H. Choi, J. W. Jung, "Fuzzy Sliding Mode Speed Controller for PM Synchronous Motors With a Load Torque Observer, " *IEEE Transactions on Power Electronic*s, vol. 27, no. 3, pp. 1530-1539, Mar. 2012.
[22] W. Xu, Y. Jiang, C. Mu, " Novel Composite Sliding Mode Control for PMSM Drive System Based on Disturbance Observer, " IEEE Transactions on Applied Superconductivity, vol. 26, no. 7, pp. 1-5, Oct. 2016.
[23] X. Zhang, Z. Li, " Sliding-Mode Observer-Based Mechanical Parameter Estimation for Permanent Magnet Synchronous Motor, " *IEEE Transactions On Power Electronics*, vol. 31, no. 8, pp. 5732-5745, Aug. 2016.
[24] B. Wang, Z. Dong, Y. Yu, G.Wang, D.Xu, " Static-Errorless Deadbeat Predictive Current Control Using Second-Order Sliding-Mode Disturbance Observer for Induction Machine Drives," *IEEE Transactions on Power Electronics*, vol.33, no.3, pp. 2395-2403, Mar.2017.
[25] T. Chen, J. Zhang, L. Peng, "Anti-load Disturbance Control Method Base on Torque Sliding Mode Observer, " *Power System Protection and Control*, vol.41, no.8, pp. 114-118, Apr.2013.
[26] S. Chi, Z. Zhang, and L. Y Xu, " Sliding-mode sensorless control of direct-drive PM synchronous motors for washing machine applications," *IEEE Transactions on Industry Application*, vol. 45, no. 2, pp. 582-490, Mar./Apr. 2009.

Wenqi Lu received the B.S.degree from Zhejiang Ocean University, Zhejiang, China, in 2005, and the Ph.D.degree from Nanjing University of Aeronautics and Astronautics, Nanjing, China, in 2011, all in electrical engineering.
In 2011, he was an Assistant Professor with the Faculty of Mechanical Engineering and Automation, Zhejiang Sci-Tech University, where he has been an Associate Professor since 2017. From 2014 to 2017, he was a Post-Doctoral Researcher with the Department of Electrical Engineering, Zhejiang University. he was a guest Researcher with the Department of Energy Technology, Aalborg University since 2017. His current research interests include the control of electric machines and mechatronic system, and its application in robot and intelligent manufacturing equipment.

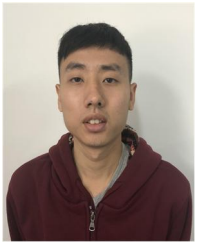

Zhenyi Zhang received the B.S.degree in mechanical and electronic engineering from the Zhejiang Sci-Tech University, Zhejiang, China, in 2016. He is currently working toward the M.S degree at Mechanical and Electronic Engineering, Zhejiang Sci-Tech University, Hangzhou, China.
His research interests include electrical motor drives, research on high speed and high precision positioning drive method of permanent magnet AC position servo system.

Dong Wang (S'13-M'16) received the B.S. degree from Zhejiang University, Zhejiang, China, in 2004, and the M.S. and Ph.D. degrees from Aalborg University, Denmark, in 2006 and 2016, respectively, all in electrical engineering.
From 2006 to 2012, he was with Grundfos R&D China, Suzhou, China, as a Senior Motor Engineer, working on the design and analysis of the permanent magnet machine and devices. From 2016 to 2017, he was a Postdoc Researcher with the Department of Energy Technology, Aalborg University, where he has been an Assistant Professor since 2017. His research interests include design and control of synchronous reluctance and permanent magnet machines.

Kaiyuan Lu (M'11) received the B.S. and M.S. degrees from Zhejiang University, Zhejiang, China, in 1997 and 2000 respectively, and the Ph.D. degree from Aalborg University, Denmark, in 2005, all in electrical engineering.
In 2005, he became an Assistance Professor with the Department of Energy Technology, Aalborg University, where he has been an Associate Professor since 2008. His research interests include design of permanent magnet machines, finite element method analysis, and control of permanent magnet machines.

This article has been accepted for publication in a future issue of this journal, but has not been fully edited. Content may change prior to final publication. Citation information: DOI 10.1109/TPEL.2018.2881217, IEEE Transactions on Power Electronics

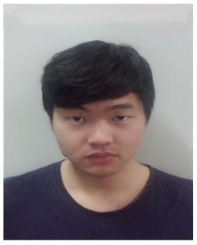

Di Wu received the B.S.degree in mechanical and electronic engineering from the Zhejiang Sci-Tech University, Zhejiang, China, in 2016. He is currently working toward the M.S degree at Mechanical and Electronic Engineering, Zhejiang Sci-Tech University, Hangzhou, China.

His research interests include electrical motor drives, research on sensorless direct power control of synchronous reluctance motor.

Kehui Ji received the B.S. degree in electrical engineering from JiangSu University, Zhenjiang, China, in 2001, and the M.S. and Ph.D. degrees from Zhejiang University, Hangzhou, China, in 2004 and 2013, respectively, all in electrical engineering.

From 2004 to 2010, he worked in industry, as a R&D Engineer, principally on the design of the permanent magnet machine and drive. Since 2013, he worked as a Lecture in Zhejiang Sci-Tech University, Hangzhou, China. His research interests include electrical machine drive and motion control system.

Liang Guo received the master's degree from Shandong University, Jinan, China, in 2003, and the Ph.D. degree from Zhejiang University, Hangzhou, China, in 2006, all in electrical engineering.

She was a Visiting Scholar with the Power Electronics and Machines Group, The University of Nottingham, Nottingham, U.K. She is currently an Associate Professor with the Faculty of Mechanical Engineering and Automation, Zhejiang Sci-Tech University, Hangzhou. Her current research interests include electromagnetic analysis and optimization of electrical machine, in particular, in permanent magnet machines.